

## **An Improvement to MODIS TPW Products by Damping the Variation of Surface Reflectance in Channel 2**

**Mohammad Reza Mobasheri<sup>1\*</sup>, Davod Ashourloo<sup>2</sup>**

Received: 2012/3/5

Accepted: 2013/1/1

### **Abstract**

Total Perceptible Water (TPW) is an important parameter in climatology and weather forecasting and is directly related to any climate process. There are three approaches to estimate this parameter i.e. using radiosonde, using GPS and calculating from satellite images where the first two are localized and the last one can give an instant view of TPW in a vast region. The algorithm used for the TPW calculation from MODIS images is related to the ratio of the reflectance in a water vapor absorbing channel and the reflectance in a non-absorbing channel. Due to strong horizontal variation in the surface reflectance in non-absorbing channels, the retrieved TPW varies strongly from one pixel to its neighboring pixels while it is believed that the horizontal gradient of TPW is very weak. To solve this problem, a damping coefficient was added to the non-absorbing channel reflectance. It is found that this coefficient differs for different surface covers. The current work presents a procedure for calculating these coefficients. The results of a comparison between modified TPW and those extracted from GPS data showed a  $R^2$  of 0.81 whilst this was about 0.67 for non-modified MODIS TPW.

**Keywords: Total Perceptible Water; GPS; Radiosonde; MODIS Images; Remote Sensing.**

---

1. Associated Professor, Remote Sensing Eng. Dept., KN Toosi University of Technology, [mobasheri@kntu.ac.ir](mailto:mobasheri@kntu.ac.ir)  
2. PhD Student, Remote Sensing Eng. Dept., KN Toosi University of Technology

The content of water vapor in a column of the atmosphere that is a measure of the Total Perceptible Water (TPW) is a result of the balance between precipitation, evaporation and convergence of humidity (Fontaine et al., 2003). TPW is an important parameter in water vapor climatology and weather variability in the lower troposphere and is directly related to any climate process. Therefore, its correct measurement with relatively high spatial resolution is important (Mobasheri et al., 2008). To continuously monitor the variability and change in atmospheric TPW, simultaneous measurements in the vast area is needed. In this regard, recent advances in satellite observations from either infrared sounders or microwave radiometers are somehow promising (Gao et al., 2004).

Accurately mapping the global atmospheric TPW is an important issue in the global energy and water cycle monitoring. However, the assessment of TPW locally can assist in weather forecasting as well as nowcasting (Mobasheri, 2004). Unfortunately, such observations still have their limitations in resolution both temporally and spatially. The poor-quality of radiosonde TPW data and lack of observation with adequate

spatial-temporal resolution makes accurate climatological studies difficult. For instance, radiosonde can provide vertical profile information regarding meteorological variables such as pressure ( $p$ ), temperature ( $T$ ), and relative humidity (RH), but not only the operational cost restricts their use, the number of observation is limited to two observations per day (Westwater et al., 2003). On the other hand, TPW is of particular importance for monitoring seasonal and annual changes in the perceptible water on regional scales particularly for drought monitoring.

Currently available infrared sounder sensors are capable of retrieving water vapor profiles as a byproduct of remote sensing of the atmospheric temperature profiles where the derived water vapor profile depends, in part, on the initial guess for the temperature and moisture profiles (Mobasheri, 2007; Rahimzadegan and Mobasheri, 2010). Remote sensing of water vapor from ground-based transmission measurements in and around the near IR absorption channels has been reported by Kaufman and Gao (2002). Also, the columnar water vapor can be derived using the ratio of the calculated reflectance at  $0.94\mu\text{m}$  and  $1.14\mu\text{m}$  water vapor absorption channels that is a differential

absorption technique for remote sensing of water vapor suggested by Frouin et al., (2003). In this technique, two water vapor channels centered at the same wavelength of (i.e.  $0.94\mu\text{m}$ ) but having different widths ( $0.17\mu\text{m}$  and  $0.45\mu\text{m}$ ) were used. A ratio of the reflectance in these two channels is claimed to be independent of the surface reflectance (Kaufman and Gao, 2002). Finally, the ratio of the reflectance in a water vapor absorption channel to the reflectance in a nearby non-absorbing channel was calibrated by Chylek et al., (2003) for TPW determination. In practice, the variation of reflectance in non-absorbing channel for different surface covers produce strong variation in the corresponding calculated TPW. In this

work, an attempt is made to reformulate this ratio to minimize the strong spatial variation in TPW.

## 2- Material and Method

### 2-1. Study Area

The study areas in this research consist of regions with different climates at different geographical location having different surface covers. These regions are confined between 24, 57, 50.3 to 43, 29, 24 northern latitudes and 43, 39, 14 to 63, 21, 11.6 eastern longitudes in Iran. A variety of climates can be found in these regions i.e. humid regions in the north and south, arid climate in the center and semiarid climate in the rest of country (Fig. 1)

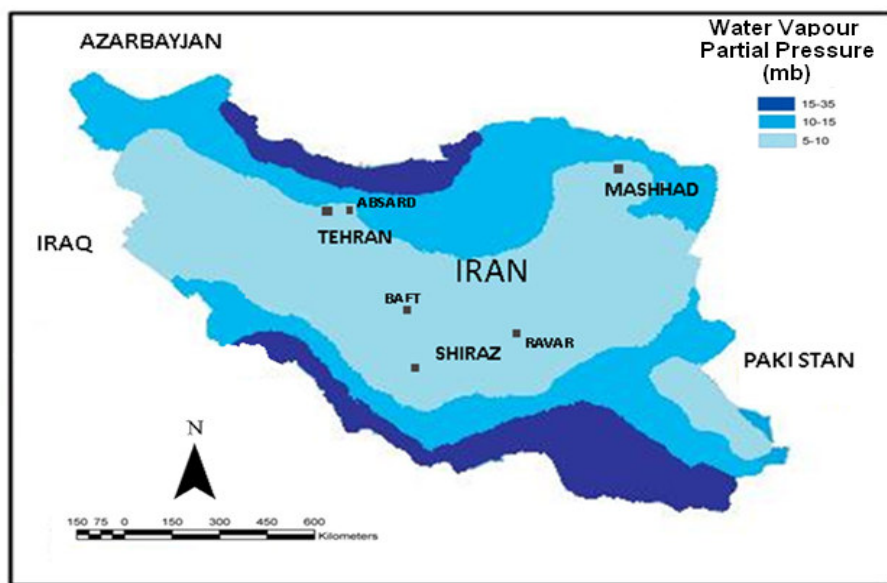


Fig 1.. Map of Annual Mean Water Vapor Partial Pressure Over the Country

## 2-2. Material and Data

### 2-2-1. Radiosonde Data

The radiosonde data were supplied from two sites, Wyoming University, USA and Iran Meteorological Organization for the duration of June 22 and July 21, 2008.

### 2-2-2. GPS Data

Atmospheric water vapor can produce a lag in signals when passing through the troposphere (equation 1). This lag is proportional to the atmospheric TPW and can be calculated accordingly (equation 2) for a hydrostatically stable atmosphere using the pressure values measured at the surface (Niell, 1996).

$$ZWD = ZPD - ZHD \quad (1)$$

$$TPW = \int ZWD \quad (2)$$

Here  $ZWD$  is Zenith Wet Delay,  $ZPD$  is Zenith Path Delay,  $ZHD$  Zenith-scaled Hydrostatic or “dry” Delay,  $\int$  is a function of physical parameters such as surface temperature, liquid water density and some gaseous constants.

### 2-2-3. MODIS TPW

42 MODIS images used in this work were acquired between June 22 and July 21, 2008. The MODIS is a sensor on board of Terra and Aqua platform collecting data in

36 different spectral channels with spatial resolution of 250 to 1000m. The acquisition time was between 10:30 to 11 for Terra and 14 to 14:30 for Aqua platform. The format of these images were HDF so using Scan Magic software, geometrical corrections based on Lambertian system with elliptical base of WGS84 by applying the nearest neighbourhood method were carried out. Since the objective of the research was retrieval of TPW, then no atmospheric corrections for water vapour was carried out.

In this research, an optical technique offered by Kaufman and Gao (1992) was used for TPW calculation. This technique is based on utilization of the solar radiation reflected on the surface and is measured by the Moderate Resolution Imaging Spectrometer (MODIS) onboard of Earth Observing platforms Terra and/or Aqua. The technique can only be applied to the cloud free images acquired over land.

In this work two channels of MODIS specifically designed for monitoring the global distribution of water vapor over land in cloud-free conditions, were selected. The technique is based on detection of the amount of absorbed solar radiation by water vapor as it passes through the atmosphere

down to the surface and back up to the sensor.

The main uncertainty in the determination of water vapor comes from the reflectance for heterogeneous surfaces in the non-absorbing channel (Kaufman and Gao, 1992; ).

The available MODIS channels offer a variety of possibilities, from a strong absorption in a narrow channel around 0.935 $\mu\text{m}$  (used for detection of water vapor in clouds), to more moderate absorption around 0.95-0.97 $\mu\text{m}$  and to a weaker absorption around 0.91 $\mu\text{m}$  (Kaufman and Gao, 1992).

Kaufman and Gao (1992) based their technique of remote sensing of water vapor on a ratio of reflectance in an absorbing to the reflectance in non-absorbing channels e.g. the ratio of the measured reflectance at 0.94  $\mu\text{m}$  to that of 0.86  $\mu\text{m}$ . Alternatively this could be the ratio of a strongly absorbing channel (e.g., a narrow channel centered at 0.94  $\mu\text{m}$ ) to that of a moderately absorbing channel (e.g., a wide channel centered at 0.94  $\mu\text{m}$ ) where it is believed that the latter technique, proposed by Frouinet *al.* (1990) significantly reduces the effect of surface reflectance on the channel

ratio. Of course this also significantly reduces the sensitivity of the channel ratio to water vapor. Kaufman and Gao (1992) then related this ratio to the total perceptible water  $W$  through some empirical relationship of the form:

$$T_w = \rho_{ab} / \rho_{non-ab} = \exp(\alpha - \beta\sqrt{W}) \quad (3)$$

here  $T_w$  is the atmospheric transmittance which is the ratio of the reflectance of absorbing channels ( $\rho_{ab}$ ) to the reflectance of non-absorbing channels ( $\rho_{non-ab}$ ).  $\alpha$  and  $\beta$  are coefficients determined through some in situ measurements. A rough values of  $\alpha=0.020$  and  $\beta=0.651$  for a mixture of all surfaces is suggested by Kaufman and Gao (1992).

In case the sun and sensor are not at the zenith, the  $W$  in equation (3) will be replaced by  $W^*$  which is related to the total perceptible water vapor  $W$  by the following equation (Kaufman and Gao, 1992):

$$W^* = W(1/\cos\theta + 1/\cos\theta_0); \quad (4)$$

Here  $\theta$  and  $\theta_0$  are viewing zenith angle and solar zenith angle respectively. The coefficients for the best fit to  $T_w$  as a function of  $W^*$  for the MODIS water vapor channels suggested by Kaufman and Gao (1992) is given in Table 1.

**Table 1** Values of  $\alpha$  and  $\beta$  for Different Absorbing and Non-absorbing Channels and for Two Viewing Angles of Nadir Viewing ( $\theta = 0, \theta_0 = 40$ ) and Off-nadir Viewing ( $\theta = 60, \theta_0 = 60$ ) (Kaufman and Gao, 1992)

	Absorbing Channel	MODIS Channel	Non-absorbing Channel	MODIS Channel	$\alpha$	$\beta$
Nadir	0.890-0.920	17	0.841-0.876	2	0.016	0.209
Off-Nadir	0.890-0.920	17	0.841-0.876	2	-0.003	0.181
Nadir	0.931-0.941	18	0.841-0.876	2	0.043	0.760
Off-nadir	0.931-0.941	18	0.841-0.876	2	-0.110	0.537
Nadir	0.915-0.965	19	0.841-0.876	2	0.036	0.426
Off-nadir	0.915-0.965	19	0.841-0.876	2	-0.024	0.342

Three different channel ratios can be used for  $T_w$  estimation in three different states of the atmosphere (Kaufman and Gao, 1992):

- i. *Dry Atmosphere* ( $W < 0.5$  cm): In this case, the reflectance ratio of channel 18 to channel 2 is recommended.
- ii. *Low to Moderate Water Vapor*: For TPW of around 2 cm in nadir or even less than 2 cm in off-nadir viewing angle, ratio of channel 19 to channel 2 is recommended to be appropriate.
- iii. *Humid Atmosphere*: For total perceptible water vapor more than 4cm in nadir viewing condition or even less than this value but for slant view and illumination conditions, the strong absorption in the

proposed 0.915-0.965 $\mu$ m channel may partially saturate, resulting in lower sensitivity to water vapor. In this case, a water vapor absorption channel in a spectral range corresponding to lower absorption i. e. 0.890-0.920 $\mu$ m is believed to be more appropriate for remote sensing of water vapor in humid conditions. This channel is located in the spectral region with minimum change in  $T_w$  (Kaufman and Gao, 1992). Table 2 summarizes the particulars of three water vapor absorption channels of MODIS channel 17, 18 and 19 and one non-absorbing channel 2. In this work we have focused our study on the use of channels 18 and 2 of MODIS.

**Table 2.** Characteristics of the MODIS Water Vapor Absorbing and Non-absorbing Channels.

Channel Status	Wavelength (nm)	Channel No.
Non-absorbing	841-876	2
Weak water vapor absorption	920-890	17
Strong water vapor absorption	941-931	18
Moderate water vapor absorption	965-915	19

Among these 4 channels, channel 2 has no sensitivity to water vapor and the radiations in other 3 channels are absorbed by water vapor but with different proportions. So the ratios of the reflectances of 17/2, 18/2 and 19/2 are suggested for humid, arid and semi-arid regions respectively (Kaufman and Gao, 1992). Using equation (2) and the appropriate reflectance ratio one can estimate the TPW through the following equation

$$W = \frac{(\alpha - L_n T_w)^2}{\beta}, \quad \text{where } T_w = \frac{\rho_{ab}}{\rho_{non-ab}} \quad (5)$$

### 3. Comparison of GPS and Radiosonde-Calculated TPW

It is believed that the radiosonde extracted TPWs are accurate enough and consequently are comparable to the GPS extracted TPWs. To see this, one month TPW values are calculated from:

i) Radiosonde data collected at 00 and 12 GMT and GPS data at the same time for two stations of Mashhad and Tehran where compared with each other (Figure 2). It can be seen that although there exists a good correlation between these two TPW data, but in both stations radiosonde reads a little higher than GPS. The discrepancies between the results of these two methods may come from non-vertical movement of radiosonde and possible weather instability at the time of sonding. However correlation of 90% between these two measurements renders the quality of GPS extracted TPWs reliable. This will be taken into consideration when comparing MODIS extracted TPW with those of extracted from GPS data.

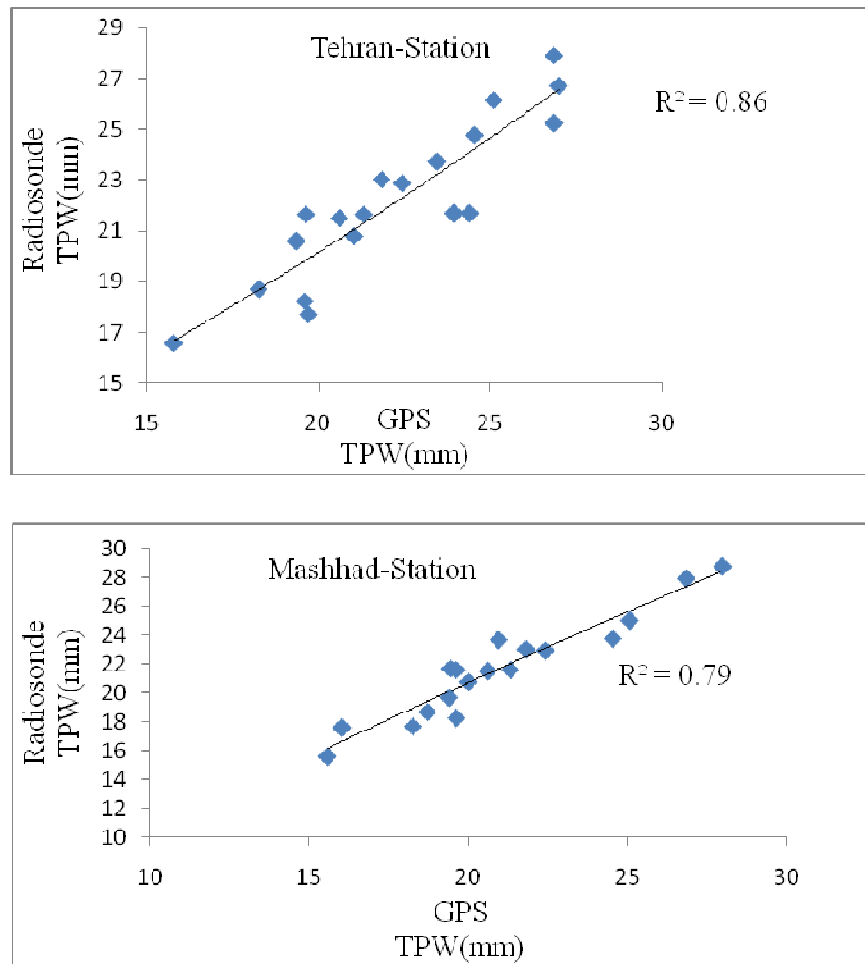


**Fig 2.** Comparison between TPW Extracted from Radiosonde and from GPS for Month of July 21 to Aug 21, 2008 at 2 Stations of Mashhad (Lower) and Tehran (Upper)

### 2-5. Comparison of GPS and MODIS-Extracted TPW

The TPWs calculated from equation (3) and those extracted from GPS data collected in 6 different stations are compared with each others. In each station, two classes of surface cover i.e. vegetation and bare soil with minimum area of 25Km<sup>2</sup> was selected.

Among these stations 2 were in humid climate, 2 in semi-arid and 2 in arid climates.

The results showed that in arid region MODIS extracted TPWs read up to 70% higher than GPS. In the humid area this reduces to 50% higher than that of GPS.



Another point to mention was the high horizontal variation of TPW in the image from one pixel to its contiguous pixels which barely happens in reality. The histograms of TPW images over two different surface covers of vegetated and non-vegetated regions for the study areas are shown in figure (3). It can be seen that this variation is higher over non-vegetated compared to vegetated surfaces. Careful investigation of channel 2 and channel 18 reflectances showed that the strong horizontal variation of TPW is due to the high variability of reflectance in non-absorbing channel 2 (Fig. 4). It can be seen in figure 4-a that the horizontal variation of reflectance in water vapor absorbing channel 18 is low due to the uniform distribution of water vapor in the atmosphere. This for channel 2 is different (Fig. 4-b) i.e. the reflectance in non-absorbing channel 2 due to the change of surface cover is highly variable and

consequently the ratio of the reflectance of these two channels are highly variable. This is believed to be the reason for poor correlation between MODIS TPW product and GPS extracted TPW for the same pixels. This is shown in figure (4-d) where the calculated TPW using equation (2) has 93% correlation with channel2 reflectance and only 10% correlation with channel 18 reflectance. These strong variations in calculated TPWs can be controlled by controlling channel 2 variations. In other words, there must be some way to minimize the dependence of the ratio of channel 18/2 to channel 2 variations for different surface covers. This is the objective of this work. This research has focused on the ratio of channel 18 to channel 2 where 17/2 and 19/2 might suffer from the same problem and must be taken care of. The reason for this selection was simply the applicability of 18/2 for the area under study.

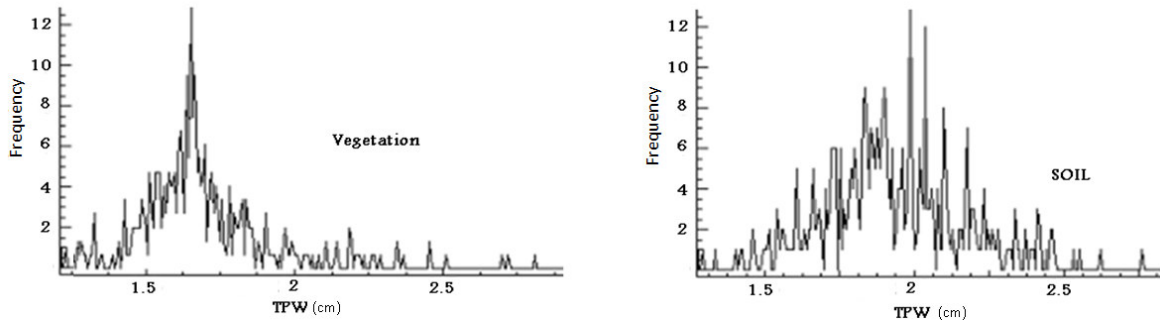


Fig 3. Histogram of Calculated TPW over Vegetated (Left) and Over Non-Vegetated (Right)

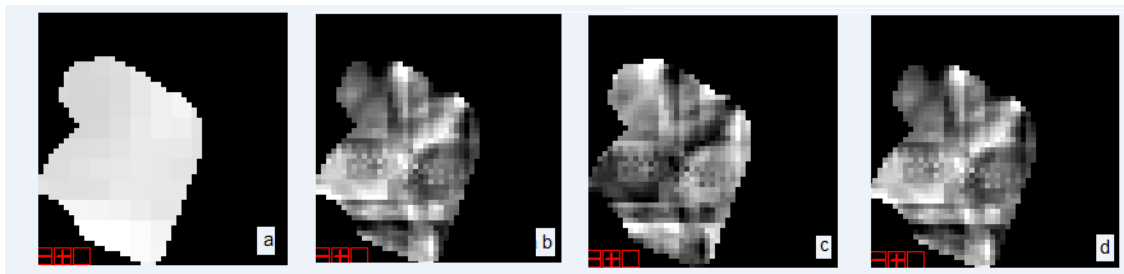


Fig 4. a- Reflectance in Channel 18, b- Reflectance in Channel 2, c- Ratio of 18/2, and d- Calculated TPW Using Equation (2).

### 3-Modification of MODIS TPW Algorithm

Due to the abovementioned problem in MODIS TPW assessment, there is a need to control the high fluctuations in TPW for adjacent pixels where it is believed to be mostly due to the fluctuation in channel 2 reflectance. A methodology for solving this problem is presented in this section and tested by using simultaneously collected MODIS and GPS TPW data.

In this methodology, equation (3) is used. The GPS calculated TPW values ( $W_{GPS}$ ) is inserted in equation (3) and the ratio of channel 18 to channel 2 reflectance ( $T_{w,GPS}$ ) was calculated for the pixel containing GPS set.

$$T_{w,GPS} = \exp(\alpha - \beta \sqrt{W_{GPS}}) = \rho_{18} / \rho_2 \dots \dots (6)$$

The scatter plot of reflectance in channels 18 and 2 for vegetated and non-vegetated surface covers are shown in Fig. (5). Also a linear fit to these data (solid

line) as well as a line with the slope of  $T_{w,GPS}$  calculated from equation (6) is shown in Fig. (5). It is found that over vegetation the MODIS TPW was 10% less than the actual values (GPS TPW) while this over non-vegetated surfaces was 10% more (Fig. 5).

As mentioned before the high fluctuation in TPW is due to the high variation in channel 2 reflectance. Now to control and ultimately minimize these fluctuations a Damping Coefficient (DC) is introduced in the denominator of equation (2) as:

$$T_w = \frac{\rho_{18}}{\rho_2 + \epsilon} \dots\dots\dots (7)$$

To model  $\epsilon$  for non-vegetated surfaces as well as vegetation covers, the GPS extracted TPWs and equation (6) is used and the  $T_{w,GPS}$  for 6 stations is calculated. Then these calculated  $T_{w,GPS}$  and  $\rho_{18}$  and  $\rho_2$  reflectances of channels 18 and 2 are inserted into equation (7) and values for  $\epsilon$  is calculated and averaged for 6 stations. These are called **Eveg** for vegetated and **Esoil** for non-vegetated surfaces (Table 3).

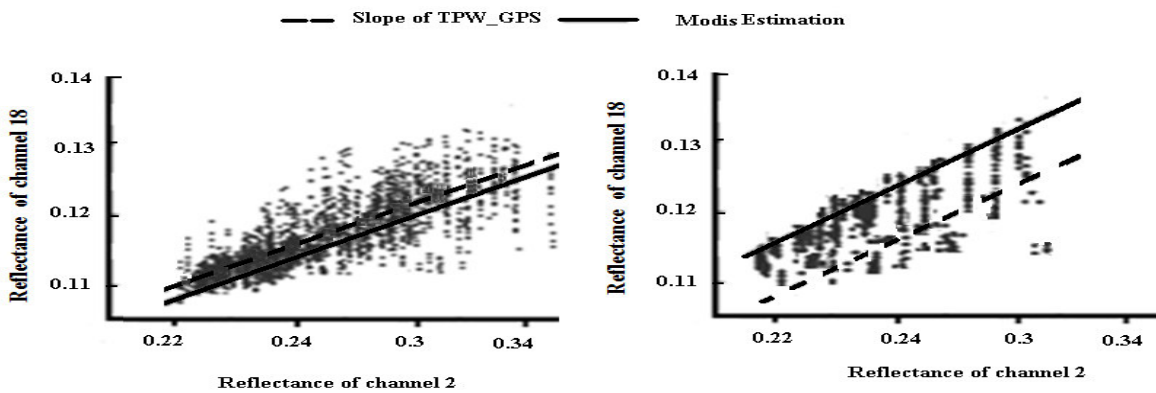


**Fig 5.** Scatter Plot of Reflectance in Channel 18 with respect to Channel 2 for Non-vegetated Surface (Right) and for Vegetation (Left). The Dashed Lines are the Calculated Slope from Equation (6) i.e.  $T_{w,GPS}$  and the Solid Lines are a Linear Fit to Data.

**Table 3.** Values of Calculated DC Averaged for 6 Stations where **Eveg** is for Vegetation-covered Surfaces and **Esoil** is for Non-vegetated Surfaces.

Station No.	Non-vegetation <b>Esoil</b>	Vegetated <b>Eveg</b>	Station No.	Non-vegetation <b>Esoil</b>	Vegetated <b>Eveg</b>
1	0.013	-0.017	4	-0.016	0.014
2	0.01	-0.014	5	-0.016	0.01
3	0.011	-0.015	6	-0.018	0.012

Using these averaged values of DC, equation (7) was applied to another 8 MODIS pixels containing GPS stations for pure vegetated and non-vegetated pixels and TPWs were calculated. It was found

that the variation of TPWs in adjacent pixels reduced dramatically. The RMSE of GPS and MODIS calculated TPWs dropped from 1.02 before correction to 0.63 after correction (Table 4).

**Table 4** Comparison of TPWs in Vegetated and Non-vegetated Surface before and after Corrections for DC.

Surface Cover	Station No.	GPS(cm)	MODIS(cm) Before Correction	MODIS(cm) After Correction
Vegetation	1	2.7	3	2.9
	2	3.1	2.8	3
	3	2.3	2.1	2.4
	4	1.68	1.85	1.56
	mean	2.45	2.63	2.46
Non-vegetated	1	2.7	3.2	3
	2	3.1	3.5	2.9
	3	2.3	2.7	2.4
	4	1.68	2.9	2.3
	mean	2.44	3.07	2.65

**Case of Mixed Pixel**

What we have in reality is mixed pixels containing different proportions of vegetated and non-vegetated surfaces (mostly bare soils). To assign a proper DC value to these mixed pixels, the fractions of

each of the vegetated and non-vegetated portion of surface in each pixel must be determined. This is done through Linear Spectral Unmixing (LSU) method as follow:

$$\rho_{\lambda} = n_1\rho_{\lambda 1} + n_2\rho_{\lambda 2} + \dots + n_i\rho_{\lambda i} \tag{8}$$

Where  $\rho_\lambda$  is the pixel reflectance calculated from MODIS,  $\rho_{\lambda_i}$  is the reflectance of the  $i$ th endmember present in the pixel with a fraction of  $n_i$ . Using known values of  $\rho_{\lambda_i}$  (for every endmembers in each channel) and adequate number of image bands one can calculate the  $n_i$  values. This is done roughly for two classes of vegetated and non-vegetated surfaces in this work. The reflectances are found by averaging over full covered vegetation and full non-vegetated pixels (bare soil) in the region of study. Then using these calculated  $n_i$  values, it is possible to build up the appropriate DC for the mixed pixel through the following mixing equation:

$$\mathcal{E} = n_1 \mathcal{E}_{veg} + n_2 \mathcal{E}_{soil} \quad (9)$$

It is evident that this method works if the reflectance of the individual endmembers is known. To evaluate the workability of this method, the fraction of vegetation and bare

soil for another region where calculated using equation (8), then using equation (9) and table (2), the DC values for the pixels under study was calculated. After that equation (7) was used to calculate the transparency of  $T_w$  and finally using equation (4) the TPWs for the region of study were calculated. The histogram of the resulting image is shown in Fig. 6 for TPWs before and after corrections. It was found that the fluctuations of TPW values in the neighboring pixels were reduced noticeably. Also the new values of TPWs are closer to the values calculated by GPS data. This is shown in figure (7) as a horizontal transect for the MODIS TPW and modified TPW. As can be seen the high fluctuations in the MODIS TPW product in the neighboring pixels is smoothed down in modified transect.

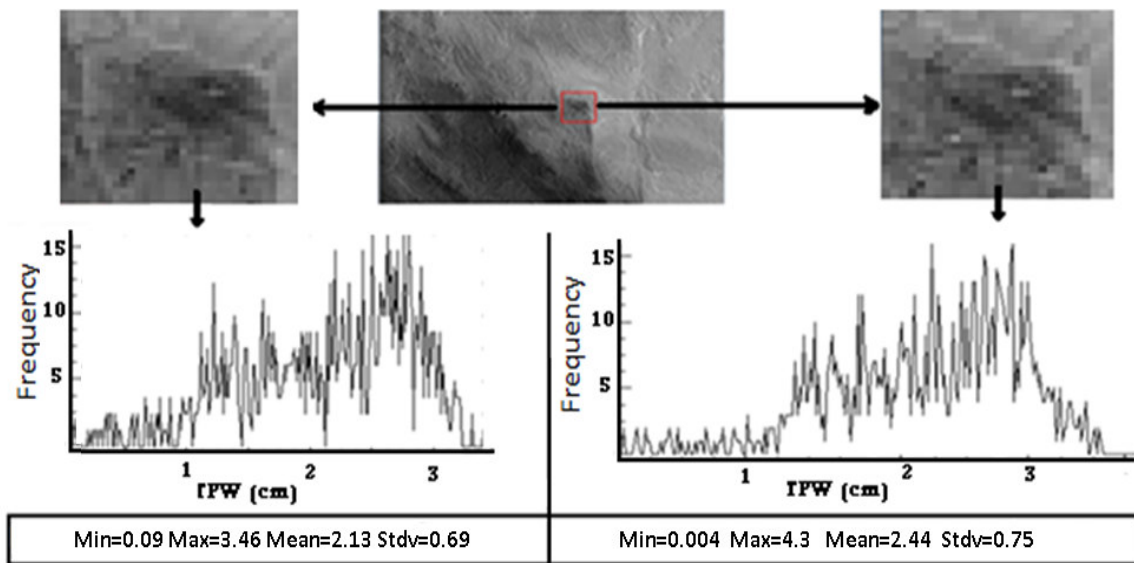


Fig 6. The Statistical Results of TPWs for MODIS Algorithm (Left) and Modified (Right)

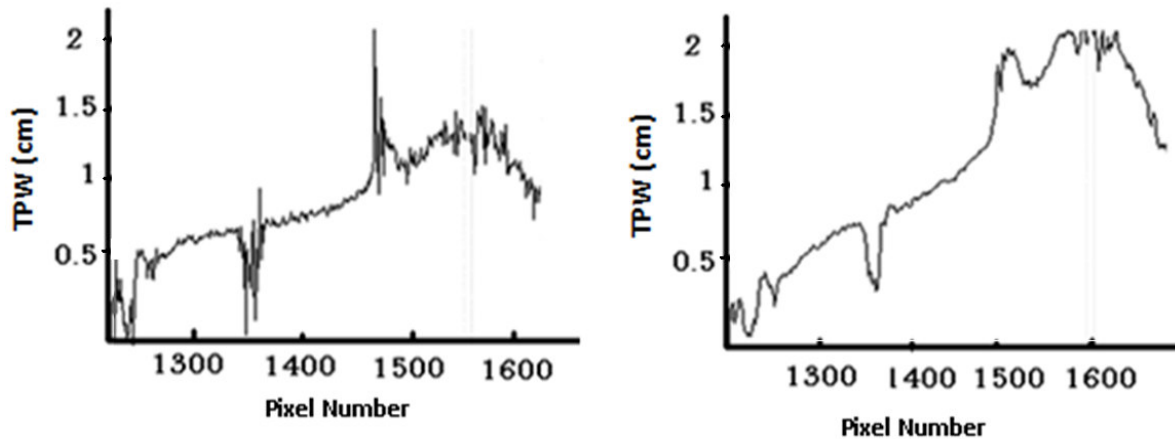
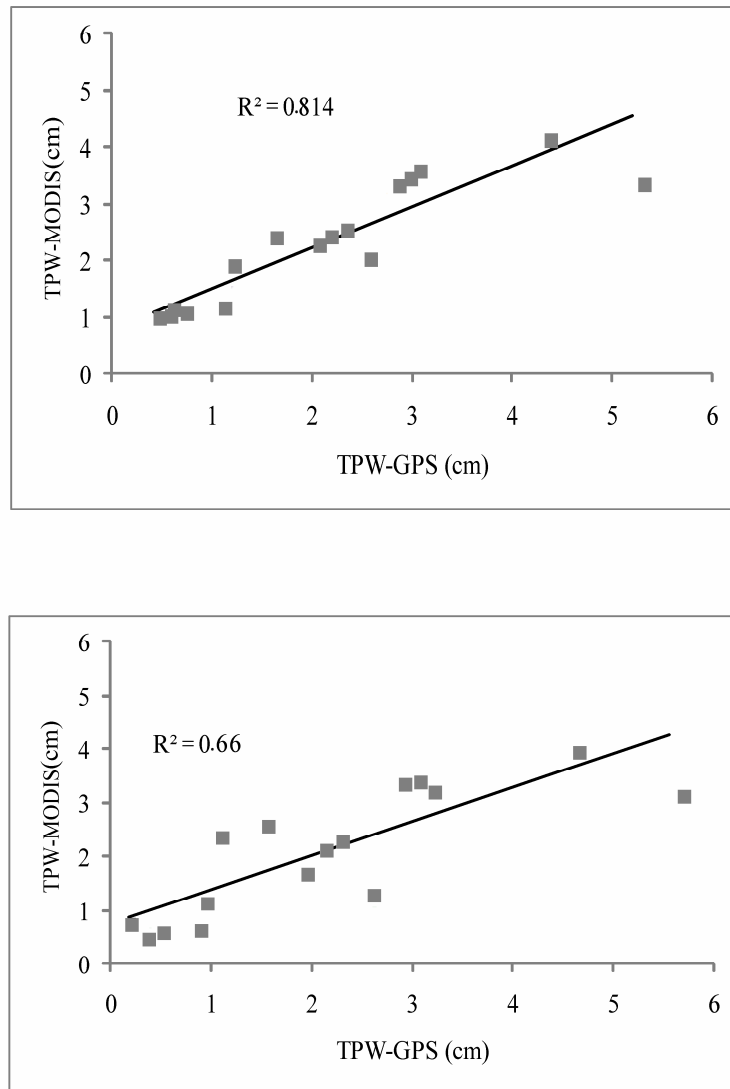


Fig 7. An Arbitrary Horizontal Profile (Transect) in the Image of MODIS TPW (Left) and Modified TPW (Right). The One in the Right Reads Closer to GPS TPW

Finally the TPW retrieved from modified algorithm and those of non-modified MODIS TPW all for those pixels containing GPS stations are compared with GPS

extracted TPWs. The results show a  $R^2$  of 0.67 between non Modified MODIS TPWs and GPS and 0.81 between Modified TPW and GPS (Fig. 8).



**Fig 8.** Comparison between TPWs Extracted from GPS with those Retrieved from MODIS Algorithm (Lower) and those Modified with our Technique (Upper).

**Conclusion**

The MODIS algorithm for calculation of atmospheric TPW is related to the reflectance ratio of one absorbing channel

(here channel MODIS 18) to a non-absorbing channel (here channel 2 of MODIS) through an empirical relation. Using this equation for TPW estimation brings some uncertainties mostly due to the

high fluctuations in surface reflectance in channel 2. This makes the retrieved TPW to strongly vary from one pixel to its neighboring pixel whereas it is believed that the horizontal gradient of TPW is not that strong to create such variations. In this work, the fluctuation in channel 2 reflectance is found responsible for strong horizontal gradient in TPWs. To overcome this difficulty a damping coefficient (DC) named  $\varepsilon$  is added to the channel 2 reflectance in order to control its strong fluctuation. This coefficient is modeled by using simultaneously measured MODIS and GPS extracted TPWs for two different land cover i.e. vegetated and non-vegetated (mainly bare soils). The DC values for the mixed pixels were calculated in two steps. First, using linear spectral unmixing for estimating the fraction of each cover and second using these fractions and appropriate DC for each of the covers to find the DC for the mixed pixels. Using these DC values, equation (7), and MODIS images of the region, the modified TPW was calculated. A comparison between the modified TPW and those extracted from GPS data showed a  $R^2$  of 0.81 while this was about 0.67 for non-modified MODIS

TPW.

## References

- [1] Chylek P, Borel CC, Clodius W, Pope PA, Rodger AP. (2003), Satellite Based Columnar Water Vapor Retrieval with the Multi-Spectral Thermal Imager (MTI). *IEEE Trans. Geosci. Remote Sens.* 41:2767–2770.
- [2] Fontaine B, Roucou P, Trzaska S. (2003), Atmospheric water cycle and moisture fluxes in the West African monsoon: mean annual cycles and relationship using NCEP/NCAR reanalysis. *Geophysical Research Letters* 30: 101029–101032.
- [3] Frouin R, Deschamps PY, Lecomte P. (1990), Determination from Space of Atmospheric Total Water Vapor Amounts by Differential Absorption near 940 nm: Theory and Airborne Verification. *J. Appl. Meteor.* 29: 448-460.
- [4] Gao BC, Chan PK, Li R R. (2004), A global water vapor data set obtained by merging the SSMI and MODIS data. *Geophysical Research Letters* 30:18103-18104.
- [5] Kaufman YJ, Gao BC. (1992), The MODIS Near-IR Water Vapor Algorithm. *IEEE Transaction on Geosciences and Remote Sensing.* 30: 876-884.
- [6] Mobasheri MR. (2007), Fundamental of Physics in Remote Sensing and Satellite Technology, Farsi (ed.). K.N.Toosi



- University of Technology Publication: Tehran, Iran. PP152-196.
- [7] Mobasheri MR. (2004), An Advanced International Course in Satellite Meteorology in Regional Meteorological Training Center (RMTC), under World Meteorological Organization (WMO), 12-23 Jun, 2004, Tehran, Iran.
- [8] Mobasheri MR, Purbagher Kordi SM, Farajzadeh M, Sadeghi Naeni A. (2008), Improvement of Remote Sensing Techniques in TPW Assessment Using Radiosonde Data, *Journal of Applied Sciences* 8:480-488.
- [9] Neill AE. (1996), Global mapping functions for the atmosphere delay at radio wavelengths, *Journal of Geophysical Research*. 101: 3227–3246.
- [10] Rahimzadegan M, Mobasheri MR. (2010), An attempt for improving MODIS atmospheric temperature profiles products in clear sky, *Meteorological Applications*. In press. DOI: 10.1002/met.221
- [11] Westwater ER, Stankov BB, Cimini D, Han Y, Shaw JA, Lesht BM, Long CN. (2003), Radiosonde humidity soundings and microwave radiometers during Nauru99, *Journal of Atmospheric and Oceanic Technique*. 20: 953–971.

## بهبود محصولات TPW سنجنده مودیس با استفاده از میرایش

### بازتابندگی سطح در باند ۲

محمد رضا مباشری<sup>۱</sup>، داوود عاشورلو<sup>۲</sup>

تاریخ دریافت: ۹۰/۱۲/۱۵

تاریخ پذیرش: ۹۱/۱۰/۱۲

آب قابل بارش کلی جو (TPW) پارامتری مهم در اقلیم‌شناسی و پیش‌بینی هوا بوده و مستقیماً با هرگونه فرآیند اقلیمی ارتباط دارد. سه روش برای تخمین این پارامتر وجود دارد، استفاده از رادیوساوند، استفاده از GPS و استخراج از تصاویر ماهواره‌ای. در دو روش اول این پارامتر نقطه‌ای محاسبه می‌شود در حالیکه در روش سوم با یک نگاه لحظه‌ای، این پارامتر در سطحی وسیع قابل محاسبه می‌باشد. الگوریتمی که در مودیس برای استخراج TPW مورد استفاده قرار می‌گیرد از نسبت بازتابندگی در یک باند جذبی بخار آب به بازتابندگی در یک باند غیر جذبی بدست می‌آید. از طرفی نظر به تغییرات شدید بازتابندگی سطحی باند غیر جذبی در پیکسل‌های مجاور، TPW محاسبه شده شدیداً از یک پیکسل به پیکسل مجاور آن تغییر می‌کند در حالیکه اعتقاد بر این است که تغییرات افقی TPW نمی‌تواند شدید باشد. برای حل این مسئله، یک ضریب میرایش (Damping) به بازتابندگی در باند غیر جذبی اضافه گردید. مشاهده شد که این ضریب به نوع پوشش سطحی حساس است. در این پژوهش روشی برای محاسبه مقادیر ضریب میرایش برای پوشش‌های مختلف ارائه گردید. نتایج TPW بدست آمده از این روش با مقادیر بدست آمده از GPS همبستگی ۰.۸۱ را نشان می‌دهد در حالیکه این مقدار برای مدل اصلاح نشده ۰.۶۷ می‌باشد.

واژه‌های کلیدی: آب قابل بارش کلی، GPS، رادیوساوند، تصاویر مودیس، سنجنش‌ازدور.

۱. دانشیار سنجنش از دور دانشگاه صنعتی خواجه نصیرالدین طوسی

۲. دانشجوی دکترای سنجنش از دور دانشگاه صنعتی خواجه نصیرالدین طوسی